

Posttranscriptional Regulation of the Breast Cancer Susceptibility Gene *BRCA1* by the RNA Binding Protein HuR

Jodi M. Saunus,¹ Juliet D. French,¹ Stacey L. Edwards,¹ Dianne J. Beveridge,³ Esme C. Hatchell,³ Sarah A. Wagner,¹ Sandra R. Stein,² Andrew Davidson,⁴ Kaylene J. Simpson,⁵ Glenn D. Francis,² Peter J. Leedman,³ and Melissa A. Brown^{1,5}

¹School of Molecular and Microbial Sciences, The University of Queensland and ²The Princess Alexandra Hospital, Woolloongabba, Queensland, Australia; ³Laboratory for Cancer Medicine, the UWA Centre for Medical Research, Western Australian Institute for Medical Research and School of Medicine and Pharmacology, The University of Western Australia and ⁴Department of Medical Oncology, Royal Perth Hospital, Perth, Australia; and ⁵Department of Biochemistry and Molecular Biology, The University of Melbourne, Victoria, Australia

Abstract

***BRCA1* is a breast cancer susceptibility gene that is down-regulated in a significant proportion of sporadic breast cancers. *BRCA1* is posttranscriptionally regulated by RNA-binding proteins, the identities of which are unknown. HuR is an RNA binding protein implicated in posttranscriptional regulation of many genes and is overexpressed in sporadic breast cancer. To investigate the possibility that these two molecules are functionally linked in breast cancer, we performed bioinformatic analysis of the *BRCA1* 3' untranslated region (UTR), RNA-protein assays with the HuR protein and the *BRCA1* 3'UTR, and immunohistochemical analysis of a cohort of breast tumors using antibodies against *BRCA1* and HuR. Here, we describe the identification of two predicted HuR-binding sites in the *BRCA1* 3'UTR, one of which binds specifically to HuR. We also show that this interaction is disrupted by single nucleotide substitutions in the *BRCA1* 3'UTR and that endogenous HuR protein associates with *BRCA1* transcripts in T47D and MCF7 breast cancer cells. Expression of ectopic HuR results in a significant decrease in *BRCA1* protein expression and also *BRCA1* 3'UTR activity. Immunohistochemical analysis revealed that although *BRCA1* and HuR expression were associated with some clinicopathologic features of the tumors, there was no statistically significant correlation between *BRCA1* and HuR protein expression. These results identify the first posttranscriptional protein regulator of *BRCA1* and have implications for understanding *BRCA1* regulation in human breast cancer.** [Cancer Res 2008;68(22):9469–78]

Introduction

BRCA1 is a large, nuclear phosphoprotein involved in the maintenance of genome integrity by regulating cell cycle checkpoints, DNA repair, and apoptosis (reviewed in ref. 1). Accordingly, its expression is tightly regulated (2, 3). *BRCA1* protein levels are reduced in most high-grade sporadic breast tumors (4), suggesting that disruption of regulatory pathways controlling *BRCA1* may contribute to tumorigenesis in these cases. Although the *BRCA1* promoter (5) and a number of associated transcription factors (6) have been identified, the identity and function of most of the

cis-sequences and *trans*-factors that regulate *BRCA1* expression are currently unknown. Down-regulation of *BRCA1* in tumors is associated with disruption of histone acetylation and *BRCA1* promoter methylation in 10% to 30% of sporadic tumors (e.g., ref. 7); however, the molecular mechanisms underlying the remaining cases is unclear. Interestingly, reduced levels of *BRCA1* protein are not always associated with reduced transcript levels (8), raising the possibility that disruption of posttranscriptional regulation may contribute in some cases.

Posttranscriptional regulation of mRNA export, stability, translation efficiency, and localization are important gene regulatory mechanisms, particularly for proteins that are required rapidly or transiently in particular environmental conditions, or in particular subcellular compartments. Many cytokines, tumor suppressor genes, and proto-oncogenes are regulated this way, for example: *EGF-R* (9); *TNF- α* (10), *TP53* (11), and *p21^{WAF1}* (12). Posttranscriptional regulation often involves interactions between *cis*-acting elements in the regulated transcripts, and RNA-binding proteins that modulate mRNA dynamics (reviewed in ref. 13). *Cis* elements are predominantly located in 5' and 3' untranslated regions (UTR), generally consist of loosely defined primary sequences within particular secondary structure contexts, and are often evolutionarily conserved (14, 15). Among the best-studied of the *cis*-acting motifs is the AU-rich element, characterized by one or more AUUUA pentamers (15, 16). Other *cis*-acting elements include AU-rich motifs (17, 18) and the β -actin zipcode (19). Several groups have developed searchable online databases for predicting posttranscriptional regulatory motifs (16, 20).

The *BRCA1* 5'UTR has been shown to play an important role in regulating *BRCA1* translational efficiency (21) and a somatic point mutation in this region has been identified in a highly aggressive, sporadic breast tumor, which dramatically reduced transcript translatability (22). The *BRCA1* 3'UTR has also been shown to be functional in previous studies by our group (3); however, the potential role of this region in breast cancer has not been investigated.

HuR is a ubiquitously-expressed RNA-binding protein that regulates the stability and translation of transcripts that function in multiple cellular pathways, such as *p21^{WAF1}* (12); *COX-2* (23), *TP53* (24), *cyclins A* and *B1* (25), and *p27* (26). A consensus binding motif for HuR has been described, which is 17 to 20 nucleotides (nts) in length, rich in uridines, and forms a stem-loop structure (27). HuR has also been implicated in cancer. Overexpression of HuR increases the tumorigenicity of human colorectal cancer cells in nude mice, whereas RNAi or antisense-mediated knockdown has the opposite effect (28). Furthermore, overexpression and cytoplasmic mislocalization of HuR correlate with tumor grade in

Requests for reprints: Melissa Brown, School of Molecular and Microbial Sciences, The University of Queensland, St Lucia, Queensland 4072, Australia. Phone: 61-7-3365-4628; Fax: 61-7-3365-4699; E-mail: melissa.brown@uq.edu.au.
©2008 American Association for Cancer Research.
doi:10.1158/0008-5472.CAN-08-1159

breast, ovarian, and colorectal cancers (29–34). One study has shown that cytoplasmic HuR is more frequent in tumors from *BRCA1* mutation carriers than in tumors from familial, non-*BRCA1* mutation carriers (34); however, the molecular basis and significance of this association is not known.

In the present study, we used bioinformatic and biochemical approaches to investigate the hypothesis that HuR is a posttranscriptional regulator of *BRCA1*. We also performed immunohistochemical (IHC) analysis on a cohort of sporadic human breast carcinomas to look for possible associations between *BRCA1* and HuR expression and other clinicopathologic variables.

Materials and Methods

3' rapid amplification of cDNA ends and sequence analysis. *Rattus Norvegicus* and *Canis Familiaris BRCA1* 3'UTR sequences were obtained by 3' random amplification of cDNA ends using previously described techniques (35). The *Bos taurus Brca1* 3'UTR sequence was assembled from expressed sequence tag [EST; CN793654 (nts 1–672), CK982254 (nts 24–695), and BI537972 (nts 357–429)] using BLAST (36). Other nucleotide sequences and ESTs were obtained from the National Center for Biotechnology *Entrez* sequence database.⁶ Vertebrate sequence conservation analysis was conducted using the University of California Santa Cruz (UCSC) Genome Browser,⁷ human AU-rich element-containing mRNA database (16), UTRResource⁸, and Transterm⁹ were used to analyze the human *BRCA1* 3'UTR (Y08864) for putative regulatory motifs. Conserved oligonucleotide motifs (14) were located manually. AU-rich sequences were also located manually, defined as adenine/uridine subsequences of at least six nucleotides, containing AUUUA. RNA secondary structure predictions were performed on the full-length *BRCA1* 3'UTR sequence (Y08864) and RNA probe sequences used in *in vitro* binding assays using Vienna RNAfold (37) with default prediction variables.

RNA protein binding assays. To make RNA probes, recombinant pGEM-T easy plasmids containing *BRCA1* 3'UTR subsequences or no insert (vector control) were linearized at the 3' end of the insert with *Sal* I or *Nco* I (Roche), and transcribed *in vitro* with T7 (sense) or SP6 (antisense) RNA polymerase (Riboprobe; Promega), in the presence of 50 μ Ci α ³²P-UTP according to the manufacturer's instructions. Full-length RNA probes were purified on 8 mol/L urea, 5% polyacrylamide gels, eluted overnight at 4°C in elution buffer (0.5 mol/L ammonium acetate and 1 mmol/L EDTA), then ethanol-precipitated, washed, and resuspended in RNase-free water.

Protein extracts were prepared from transfected HeLa cells using radioimmunoprecipitation assay (RIPA) lysis buffer as previously described (38). Analysis of RNA protein interactions was performed by RNA-electrophoretic mobility shift assay (REMSA) as described (3). Protein extracts (5 μ g) were incubated with RNA probes (1×10^5 cpm determined by scintillation counting) at room temperature for 20 min. Unprotected RNA was degraded with 5 μ L REMSA stop solution [RNase-T1 (Sigma-Aldrich; 5 U/ μ L), heparin (20 μ g/ μ L), 60% glycerol, and 0.1% bromophenol blue]. For supershift experiments, 350 ng of a HuR-specific antibody (3A2; Santa Cruz Biotechnology) were added to binding reactions for 45 min on ice, before the stop solution. RNase-resistant RNA-protein complexes were resolved on native 5% polyacrylamide gels and imaged by autoradiography. For UV cross-linking, RNA-protein reactions were processed identically to REMSA reactions (using stop solution without glycerol or bromophenol blue), then treated with UVC radiation (3×10^5 μ J; 254 nm) for 5 mins on ice, 1 cm from the source. Unlinked RNA was then degraded with RNase A (Sigma; 100 μ g/mL) for 10 min at 37°C. Proteins linked to radiolabeled RNA were resolved by SDS-PAGE, and then imaged by autoradiography.

Site-directed mutagenesis. Single nucleotide mutations were introduced into a pGEM-T easy plasmid containing *BRCA1* 3'UTR nucleotides

281 to 315 using the QuikChange mutagenesis kit (Stratagene) according to the manufacturer's instructions. Plasmids were sequenced across the insert by the Australian Genome Research Facility to validate sequence changes (data not shown).

Immunoprecipitation-reverse transcription PCR. Immunoprecipitation-reverse transcription-PCR (IP-RT-PCR) assays were performed as previously described (12) except that extracts were from MCF7 and T-47D breast cancer cells. PCR was performed for 30 cycles, with annealing at 55°C using *BRCA1*-specific primers: ex20F (5'GAAGTCAGAGGAGATGTG) and ex24R (5'CAGTAGTGGCTGTGGGGG). PCR products were resolved on ethidium bromide-stained 1.5% agarose gels.

Cell culture and transient transfections. Cervical adenocarcinoma HeLa cells [American Type Culture Collection (ATCC) #CCL-2], human mammary ductal carcinoma T-47D cells (ATCC #HTB-133), and human breast adenocarcinoma MCF7 cells (ATCC #HTB-22; provided by Mike Waters, The University of Queensland Brisbane, Australia) were cultured according to manufacturer's recommendations. HeLa cells in 6-well plates were transfected with 0.5 μ g pFLAG-CMV2 (Sigma-Aldrich) empty vector or an equimolar amount of pFLAG-CMV2-HuR expression constructs using Lipofectamine 2000 (Invitrogen). Transgene expression time was 48 h.

Northern analysis. Total RNA was harvested using TriZOL (Invitrogen) according to manufacturer's instructions. RNA was detected by Northern analysis, imaged by Phosphorimaging (Typhoon 9400; Molecular Dynamics), and quantified using ImageQuant software (V 5.0; Molecular Dynamics). *BRCA1* mRNA levels were normalized to 18S rRNA and expressed as percentages of the appropriate control. Statistical analysis was performed using paired, two-tailed *t* tests.

mRNA stability analysis. *BRCA1* mRNA stability was determined by measuring the amount of mRNA at various time points after addition of the transcription inhibitor Actinomycin D (ActD). ActD was added 48 h posttransfection with HuR plasmid (see above), and *BRCA1* mRNA levels were measured at 0, 1, 2, 4, 6, and 8 h posttreatment by Northern analysis as described above. Membranes were imaged as described above. mRNA half-lives were calculated by linear regression analysis and paired, two-tailed *t* tests were used to determine the statistical significance of any differences, with *P* values <0.05 considered significant.

Western analysis. Whole-cell protein extracts were prepared using RIPA lysis buffer as above, resolved on Tris-acetate 3% to 8% polyacrylamide gels (Invitrogen), and *BRCA1* protein levels were analyzed relative to β -actin by Western analysis as previously described (38). Membranes were probed with an anti-HuR antibody (3A2; Santa Cruz Biotechnology; 1:3,000 dilution in 5% skim milk/0.1% TBS-tween 20). Detection was performed with a peroxidase-conjugated anti-mouse antibody (Amersham Pharmacia Biotech) diluted 1:10,000. Protein-antibody complexes were visualized with the enhanced chemiluminescence system (Amersham Pharmacia Biotech).

Luciferase reporter assays. Luciferase reporters used were a pGL3-basic (Promega) *BRCA1* promoter-luciferase construct (35), and a *BRCA1* 3'UTR-luciferase reporter construct, made by ligating the full-length *BRCA1* 3'UTR downstream of the luciferase coding sequence in the pSG5 vector (Stratagene). HeLa cells in 24-well plates were transiently transfected with equimolar amounts of luciferase reporter constructs (not exceeding 400 ng), plus 100 ng pFLAG-CMV2 or an equimolar amount of pFLAG-CMV2-HuR, and 20 ng *Renilla* luciferase. After 24 h of luciferase expression, *Firefly* luciferase reporter activity was determined relative to *Renilla* using a Dual Luciferase Reporter Assay kit (Promega) and a Wallac Micro β Trilux Luminometer (EG & G Wallac), according to manufacturer's instructions.

Breast tumor study population. IHC analysis was performed on tumors from consenting patients from the Princess Alexandra Hospital in Brisbane, Australia, using protocols approved by local Human Ethics committees. The study cohort consisted of 97 patients whose breast tumor tissue was surgically removed for diagnostic and/or treatment purposes during 1993 to 1994 and for which IHC staining of *BRCA1* and HuR was successful, and the majority of which had other clinical information available. This information available from clinical records is summarized in Table 1.

Tissue microarrays. Breast tissue biopsies were formalin fixed and paraffin embedded (FFPE) using standard techniques, and tumor tissue was distinguished from surrounding normal tissue in H&E-stained sections

⁶ <http://www.ncbi.nlm.nih.gov/>

⁷ <http://genome.ucsc.edu/cite.html>

⁸ <http://bigghost.area.ba.cnr.it/BIG/UTRHome/>

⁹ <http://guinevere.otago.ac.nz/transterm.html>

of each biopsy by a qualified breast pathologist (G.D.F). Tumor tissue cores (0.6 mm) were punched from donor blocks and inserted into two recipient blocks, each containing 145 cores, using a semiautomated tissue microarrays (TMA) instrument (Galileo; Beecher Instruments) and ISETMA software (V1.8; Beecher Instruments). At least 25 cores of normal surrounding tissue from selected biopsy blocks were also inserted into each TMA to serve as reference controls during histopathologic examination.

Immunohistochemistry, histopathologic examination, and statistical analysis. Sections (5 μ m) were cut from the TMA blocks containing 97 tumor samples (Table 1), transferred on to glass slides, deparaffinized, subjected to antigen-retrieval in citrate buffer in a pressure cooker for 5 min, then immunostained using anti-BRCA1 [MS110 (Ab-1); Calbiochem; 1:150 dilution] and anti-HuR [sc-5261 (3A2); Santa Cruz Biotechnology; 1:500 dilution] antibodies, and counterstaining with weak hematoxylin. The specificities of both antibodies had been previously characterized and published for use in IHC on FFPE tissues (4, 29, 30), and our staining protocols were first optimized on test sections. Staining was performed using MACH 4 (Biocare Medical) according to manufacturer's instructions. Staining was visualized using a Cardassian 3,3'-diaminobenzidine (Biocare Medical).

Analysis of stained sections was performed by a qualified and experienced pathologist (G.D.F). The presence of tumor tissue was first confirmed by examining the hematoxylin counterstain, then all tumor spots were given a score for BRCA1 or HuR expression, calculated from the overall staining intensity and the proportion of cells stained. HuR and BRCA1 expression scores were then aligned with other clinicopathologic variables in a patient database (summarized in Table 1). For descriptive purposes only, patients were categorized into negative/weak expression (scores 0–4),

moderate expression (scores 5–7), and strong expression (scores 8–9). Given the number of clinical variables in our database, we used a multiple linear regression model to mine the data set for associations using the BRCA1 or HuR score as the dependent variable. *P* values of <0.05 were considered significant. Regression analysis was performed using the statistical package Statistica (V7; Statsoft).

Results

The BRCA1 3'UTR contains a predicted HuR binding sequence. We have previously shown that *BRCA1* is posttranscriptionally regulated and that RNA-binding proteins associate with the *BRCA1* 3'UTR in a cell cycle-dependent manner (3). In an attempt to identify the *cis*-elements and *trans*-factors responsible for this activity, we performed a comprehensive bioinformatic analysis of the *BRCA1* 3'UTR, including an orthologous sequence comparison, RNA secondary structure prediction, and 3'UTR motif prediction analysis. We also conducted manual searches for three other types of regulatory motif: (a) AU-rich sequences containing AUUUA pentamers; (b) a collection of oligonucleotide motifs that are significantly overrepresented in sets of orthologous 3'UTRs compared with 5'UTRs and coding sequences, suggesting a possible generic regulatory function (14); and (c) putative HuR-binding sites. The criteria used for predicting putative HuR-binding motifs were as follows: primary sequence corresponding to the published motif (27) and that the sequence is predicted to form a stem-loop structure, which was also an important feature of the published motif. This analysis revealed a general region of interest located between nucleotides 250 and 350 of the *BRCA1* 3'UTR (summarized schematically in Fig. 1), which we named the putative regulatory region (PRR). It is highly evolutionarily conserved (Fig. 1A and C), enriched with conserved oligonucleotide motifs (Fig. 1B), contains two AU-rich regions (Fig. 1B) and two putative HuR-binding motifs (Fig. 1B and C), one of which is evolutionarily conserved (*pHuR-2*; Fig. 1C). The predicted stem-loop structures formed by the HuR-binding motifs are shown in Fig. 1D. The PRR was also predicted to contain a differentiation control element (DICE) motif (Fig. 1B); however, this element was not conserved across species and evidence suggests functional DICE motifs normally occur in multiple copies (39).

The predicted HuR binding sequence in the BRCA1 3'UTR forms RNA protein complexes with proteins including HuR. To address the validity of the predicted HuR-binding motifs (*pHuR-1* and *-2*), we conducted *in vitro* REMSA. As shown in Fig. 2B, the minimal requirements for RNA protein complex (RPC) formation were contained within *BRCA1* 3'UTR nucleotides 281–315, which corresponds to *pHuR-2* plus 15 nucleotides of downstream sequence. Interestingly *pHuR-2* alone (the 281–301 probe) was not sufficient for RPC formation.

To test whether HuR was contained within the RPCs, a HuR-specific antibody was used in a super-shift assay. This resulted in a slower-migrating complex (Fig. 3A, SS), which was even more strongly detected when protein extracts from HeLa cells expressing ectopic HuR were used. To test whether the association by HuR was direct (RNA-HuR interaction) or indirect through another RNA-binding protein, we performed UV-cross-linking analysis on protein extracts of empty vector and pFLAG-HuR transfectants with analysis of the RNA-linked proteins by SDS-PAGE. As shown in Fig. 3B (i), a 36-kDa protein (equivalent to the size of endogenous HuR) was detected using extracts from pFLAG-transfected cells, whereas a slightly larger protein corresponding to the size of FLAG-tagged, ectopic HuR, was very strongly detected using

Table 1. Characteristics of the study cohort

	No. of patients (%)		
BRCA1 staining	Negative/weak	25	25.8
	Moderate	39	40.2
	Strong	33	34
HuR staining*	Negative/weak	4	4.2
	Moderate	21	22.1
	Strong	70	73.7
Disease onset (Median age, 52 y)	Early (<50 y)	35	36.1
	Late (>50 y)	62	63.9
Tumor grade*	I	27	30
	II	36	40
	III	27	30
Tumor size*	≤20 mm	44	53
	>20 mm	39	47
Nodal status*	Negative	35	47.3
	Positive	39	52.7
CK14 status*	Negative	86	91.5
	Positive	8	8.5
CK5/6 status*	Negative	52	55.3
	Positive	42	44.7
ER status*	Negative	27	28.7
	Positive	67	71.3
PR status*	Negative	31	33.33
	Positive	62	66.67
HER2 status*	Negative	48	52.2
	Positive	44	47.8
Other patient characteristics (not included in multiple regression analysis):			
Tumor type*	Ductal carcinoma	80	85.1
	Lobular carcinoma	10	10.6
	Other	4	4.3

*For some patients, not all clinical information was available.

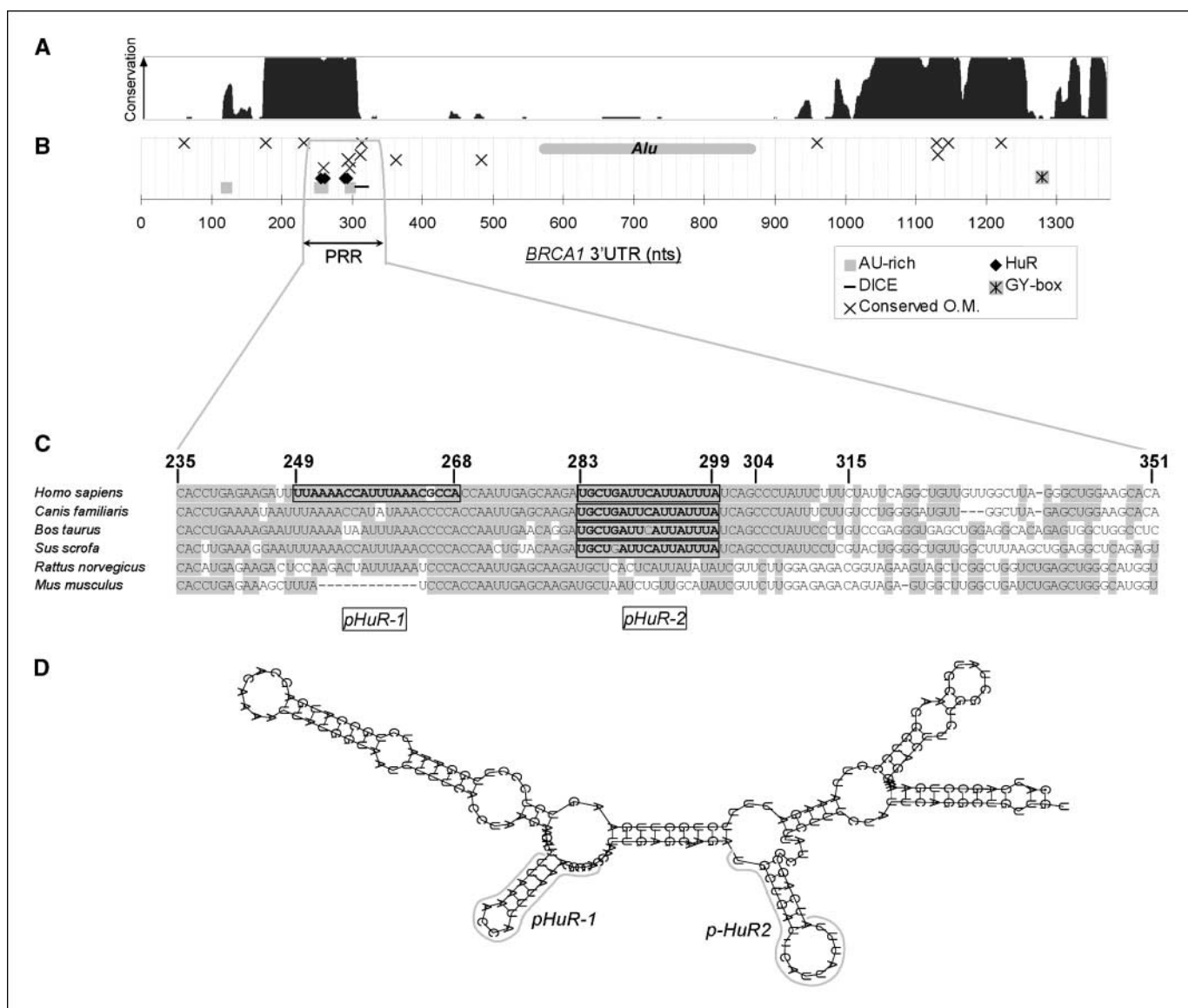


Figure 1. The *BRCA1* 3'UTR contains evolutionarily conserved sequence motifs, including putative HuR-binding sites. **A**, vertebrate Multiz conservation plot (from UCSC genome browser; see Materials and Methods) indicating the degree of evolutionary conservation of *BRCA1* 3'UTR sequences (relative to the human orthologue). **B**, distribution of conserved oligonucleotide motifs (*conserved O.M.*) and putative regulatory elements predicted using manual searching or 3'UTR regulatory motif search tools (see Materials and Methods). An *Alu* repeat element is shown for reference. A conserved subsequence surrounding a cluster of putative regulatory motifs (235–351) was selected for further analysis. Nucleotides (*nts*) are numbered from the first nucleotide after the stop codon. **C**, evolutionary *BRCA1* 3'UTR sequence comparison. The human *BRCA1* 3'UTR sequence (Entrez accession Y08864) was aligned against the orthologues listed using BLAST and ClustalW alignment tools. Gray, conserved nucleotides. Human 3'UTR nucleotide positions are indicated for reference. The two putative HuR-binding motifs (*pHuR-1* and -2) are outlined. **D**, predicted *BRCA1* 3'UTR RNA secondary structure surrounding the *pHuR* motifs. Solid gray lines, predicted stem-loop structures formed by the HuR-binding motifs are indicated by.

extracts from pFLAG-HuR transfectants [Fig. 3B (ii)]. These results suggest that HuR is one of the proteins within *BRCA1* 3'UTR RPCs, and that it binds directly to nucleotides 281–315.

To further characterize the HuR binding region in the *BRCA1* 3'UTR, we introduced several single nucleotide changes into the 281 to 315 probe and tested the protein-binding capacity with and without addition of the HuR antibody. Two of the mutated probes (289U→G and 293U→G) had significantly reduced protein-binding activity, including reduced binding in supershift assay performed with a HuR antibody (Fig. 3C). We also verified the specificity of this interaction using recombinant HuR protein, which associated with the probe, whereas an unrelated recombinant RNA-binding protein

(poly CMP-binding protein-1; CP1) did not (data not shown). Notably, nucleotides 289 and 293 are both located in the predicted loop structure formed by the *pHuR-2* motif and the 289U?G mutation is predicted to change the size of this loop (Fig. 3D).

Endogenous HuR and *BRCA1* mRNA are binding partners.

The results of *in vitro* RNA-protein binding assays strongly suggest an association between exogenous HuR and *BRCA1* RNA probes. To determine whether this association also occurs between endogenous HuR protein and *BRCA1* transcripts, we performed an IP-RT-PCR assay. Using an anti-HuR antibody and *BRCA1*-specific primers, we were able to show that endogenous HuR coimmunoprecipitates with *BRCA1* mRNA in MCF7 and T-47D

breast cancer cells (Fig. 4, *beads*). Conversely, *BRCA1* PCR products were undetectable using antibodies against the unrelated protein Glutathione-S-transferase (GST), or unrelated RNA-binding protein CP1, or when no antibody was used. PCR products were amplified from all supernatants after the IP, indicating that the negative IP results were not simply due to an absence of *BRCA1* mRNA in those extracts (Fig. 4, *S/N*). PCR products were undetectable in control lanes (Fig. 4; *no RT*), indicating that amplification was RNA dependent. These results provide clear evidence that HuR associates with *BRCA1* mRNA in the breast cancer cell lines MCF7 and T-47D.

HuR regulates *BRCA1* posttranscriptionally. Given that HuR associates with *BRCA1* mRNA *in vitro* and in breast cancer cell lines, we hypothesized that HuR may regulate *BRCA1*. To address this possibility, we investigated the effect of overexpressing HuR on the regulation of *BRCA1* mRNA stability, mRNA levels, protein expression, and 3'UTR function. As shown in Fig. 5A, expression

of ectopic HuR in HeLa cells resulted in a slight increase in endogenous *BRCA1* mRNA stability (half-life from 6.29–7.04 hours), although this was not statistically significant. Consistent with this, we found no significant difference in *BRCA1* mRNA levels (Fig. 5B). Overexpression of HuR did however result in a significant decrease in *BRCA1* protein levels in HeLa cells (Fig. 5C). This was observed in multiple independent experiments and was not associated with any change in *BRCA1* protein stability (data not shown). We also tested the effect of HuR on *BRCA1* 3'UTR activity and observed a decrease in luciferase reporter activity to ~42% compared with cells not expressing ectopic HuR ($P < 0.0001$; Fig. 5D). Taken together, our results suggest that ectopic HuR regulates *BRCA1* posttranscriptionally and that it is likely to be mediated, at least in part, by the *BRCA1* 3'UTR. Furthermore, the data raise the possibility that HuR negatively regulates *BRCA1* translation.

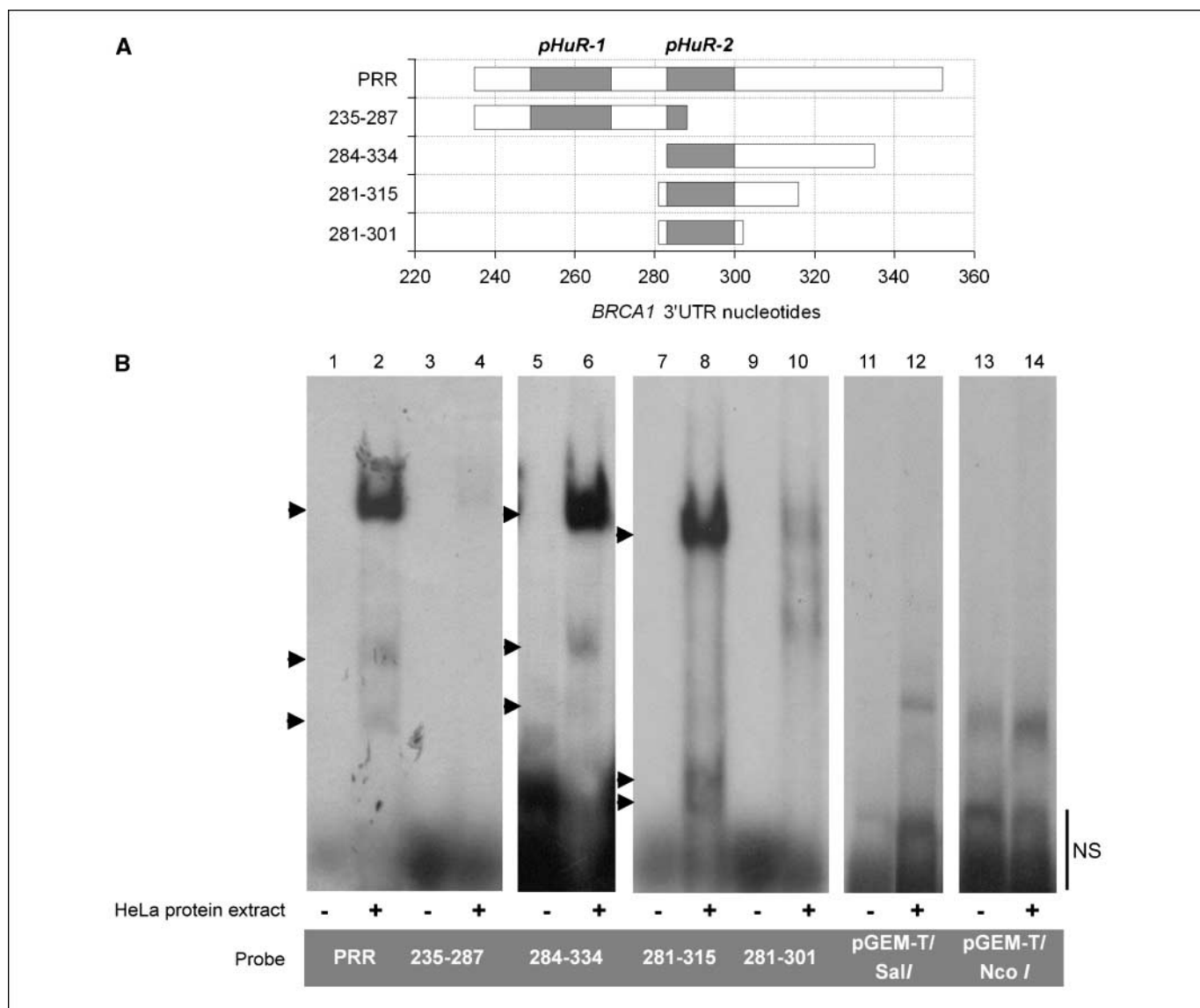


Figure 2. *BRCA1* 3'UTR subsequences form RPCs. **A**, schematic showing *BRCA1* 3'UTR subsequences tested for protein-binding activity. Nucleotides are numbered from the first nucleotide after the stop codon. Gray, relative positions of the putative HuR-binding motifs (*pHuR-1* and *pHuR-2*). **B**, REMSAs showing specific RPC (arrowheads) by *BRCA1* 3'UTR RNA probes (lanes 1–10) compared with empty vector controls (lanes 11–14). NS, free riboprobe or nonspecific-binding complexes. Equal amounts of HeLa protein extract (+) or no protein (–) were incubated with radiolabeled RNA probes (equal activities), and any RPCs that formed were resolved by native PAGE, then imaged by autoradiography.

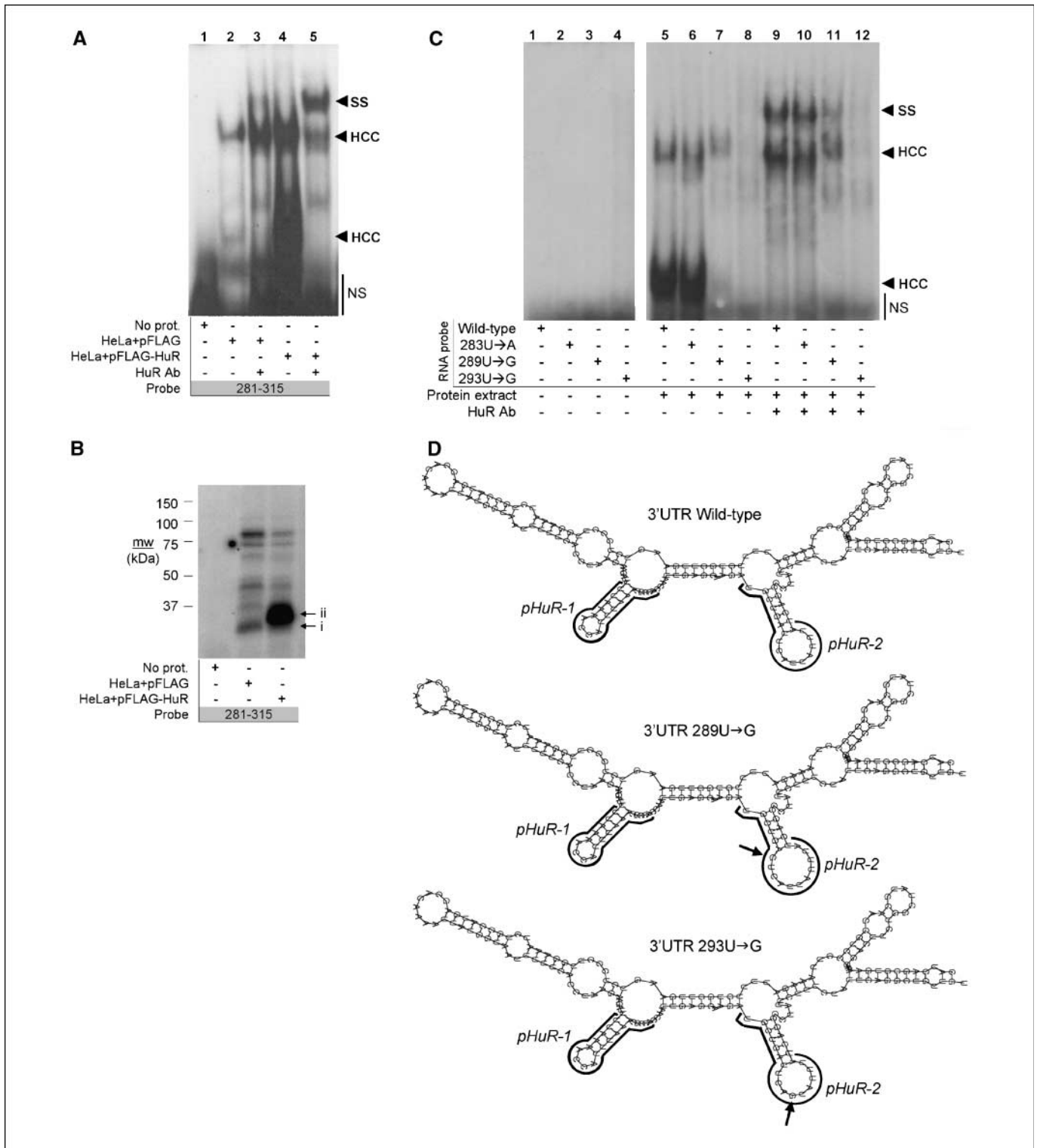
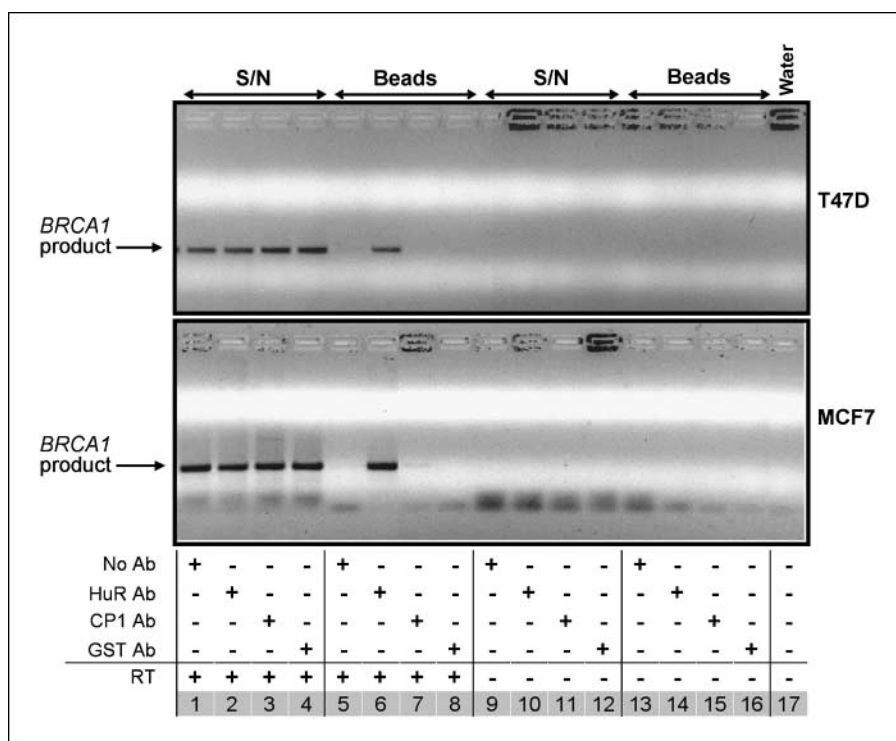


Figure 3. *BRCA1* 3'UTR RNA-protein complexes contain HuR. **A**, supershift-REMSA analysis with the *BRCA1* 3'UTR 281-315 probe. Equal amounts of radiolabeled 281-315 RNA probe were incubated with equal amounts of protein extracts from pFLAG- or pFLAG-HuR-transfected HeLa cells. A HuR-specific antibody was added to reactions 3 and 5. Any RNA protein or RNA protein-antibody complexes that formed were resolved by native PAGE, then imaged by autoradiography. *Arrowheads*, a HuR-containing complex in reaction 4 (HCC), and a higher molecular weight complex in the reactions containing the anti-HuR antibody (SS). *NS*, free riboprobe or nonspecific-binding complexes. **B**, SDS-PAGE analysis of proteins in *BRCA1* 3'UTR RPCs. Equal amounts of the 281 to 315 probe were incubated alone (*no prot.*), or with equal amounts of protein from pFLAG or pFLAG-HuR transfectants. RPCs were then covalently linked by UVC irradiation, and proteins cross-linked to the radiolabeled probe were resolved by SDS-PAGE. *Arrows*, proteins corresponding to the masses of endogenous (*i*) and FLAG-tagged HuR (*ii*). **C**, analysis of RPC formation by mutated 281 to 315 sequences relative to wild-type sequence by REMSA. Assays were conducted as above using either wild-type or mutated 281-315 RNA probes, and protein extracts from pFLAG-HuR transfectants. *Arrowheads*, HCC and complexes that were supershifted by addition of the HuR antibody. *NS*, free riboprobe or nonspecific-binding complexes. **D**, predicted *BRCA1* 3'UTR RNA secondary structure after mutagenesis of nucleotides 289U→G or 293U→G and compared with the wild-type. *Arrows*, mutated nucleotides. *Solid gray lines*, predicted stem-loop structures formed by the HuR-binding motifs.

Figure 4. HuR protein and BRCA1 mRNA are endogenous binding partners. Representative HuR/BRCA1 mRNA IP-RT-PCR experiment. Cytoplasmic extracts from MCF7 and T47D breast cancer cells were incubated with no antibody (lanes 1, 5, 9, and 13), anti-HuR (lanes 2, 6, 10, and 14), anti-CP1 (lanes 3, 7, 11, and 15), or anti-GST (lanes 4, 8, 12, and 16) antibodies (Ab), and the resulting immune complexes were precipitated using protein A and G beads. Copurifying RNA was amplified by RT-PCR using BRCA1-specific primers. RNA that was not bound to immunoprecipitated material (S/N; lanes 1–4) was used as a positive control to verify the presence of BRCA1 mRNA in the extracts. IP-RT-PCR with beads alone (lane 5), no reverse transcriptase (lanes 9–16), and water alone (lane 17) were included as negative controls. Arrow, a BRCA1-specific PCR product.



Association of BRCA1 and HuR protein expression with clinicopathologic variables in sporadic breast cancer patients.

BRCA1 and HuR are both dysregulated in a significant proportion of breast cancers (4, 31). Given our *in vitro* data indicates HuR regulates BRCA1 expression, we decided to investigate if there is an association between the expression of these two proteins in breast tumors, by performing immunohistochemistry (IHC) analysis on a cohort of 97 sporadic breast tumors using tumor microarray (TMA) (Fig. 6). The clinical cohort had a median age of 52 years with ~2/3 over 50 years, and an even distribution of tumor in all pathologic grades. The clinical samples were mostly ductal carcinomas (85%) and included patients with and without nodal disease, which were predominantly estrogen receptor (ER) positive (~71%) and progesterone receptor positive (~67%; Table 1). BRCA1 and HuR protein expression levels were scored semiquantitatively (see Materials and Methods). We found that ~26% of all patients showed negative or weak BRCA1 staining, 40% had moderate staining, and 34% stained strongly with the BRCA1 antibody. For HuR, only 4% stained weakly, 22% moderately, and the majority (74%) showed strong HuR immunoreactivity (Fig. 6A). Using a multiple linear regression model, we found significant associations between BRCA1 expression and ER expression and tumor grade (Fig. 6B). However, we did not observe any significant associations between BRCA1 expression and HuR staining intensity, or other disease or tumor features. Using HuR as the dependent variable, high HuR expression was significantly associated with tumor grade, and also with HER2 negativity. No association with BRCA1 staining, or other disease or tumor features, was evident.

Discussion

Somatic mutation of the BRCA1 gene is a rare event in breast cancer development, yet BRCA1 protein levels are reduced in a significant number of high-grade sporadic breast tumors, suggesting

that regulatory defects in BRCA1 may be important in sporadic breast cancers. Disruption of histone acetylation and BRCA1 promoter methylation is associated with down-regulation of BRCA1 in 10% to 20% of sporadic tumors; however, the mechanisms underlying down-regulation in the majority of sporadic cases are currently unknown. We have previously shown that BRCA1 can be regulated posttranscriptionally and that a number of RNA binding proteins associate with the BRCA1 3'UTR in a cell cycle-dependent manner (3). In this paper, we sought to comprehensively analyze the 3'UTR of BRCA1 in an attempt to identify critical cis-active elements and putative trans-acting proteins that can regulate BRCA1 and whose disruption in sporadic breast tumors could account for the reduced BRCA1 protein levels in these cases.

Bioinformatic analysis of the BRCA1 3'UTR revealed the presence of predicted HuR-binding sites. Our predictions of HuR-binding sites (pHuR-1 and pHuR-2; Fig. 1C and D) were based on a previously described motif, which was computationally derived from a set of mRNAs that copurified with HuR, then experimentally validated (27). In this study, *in vitro* validation experiments showed that pHuR-2, but not pHuR-1, bound specifically and directly to a group of RNA-binding proteins (Fig. 2), one of which was HuR (Figs. 3 and 4). Interestingly however, pHuR-2 alone was not sufficient for HuR binding, with the minimal probe tested (nts 281–315) including an extra 15 nt of downstream sequence. Secondary structure analysis predicts that the 281 to 315 sequence forms a full stem-loop structure. Notably, the predicted structures of pHuR-1 and pHuR-2 are the same in the contexts of the full-length 3'UTR sequence, and mutations of nucleotides predicted to map to the pHuR-2 loop abrogate HuR binding (Fig. 3D). Therefore, our data suggests a stem-loop structure is likely to be an important requirement for HuR binding, consistent with the findings of López de Silanes and colleagues (2004).

We also show that BRCA1 is posttranscriptionally regulated by ectopic HuR in HeLa cells (Fig. 5). Transcription and transcript

half-life studies indicated minimal if any changes in mRNA stability or transcript levels but a significant decrease in BRCA1 protein, raising the possibility that HuR negatively regulates BRCA1 translation. There is certainly precedence for a translation inhibitory role of HuR; for example, HuR expression negatively regulates the translation of p27 and Wnt-5a (26, 40).

HuR binds several mRNAs implicated in tumorigenesis, including Cox-2 and p27 (23, 26), and has been shown to promote cell

proliferation, migration, and invasion (41). Most relevant to the present study is the demonstration that HuR is overexpressed in a significant number of primary human breast cancers (29, 30). To determine whether overexpression of HuR correlates with low BRCA1 protein levels in the same tumors, we analyzed the expression of both proteins in a cohort of breast tumors and compared the expression with a number of clinical features using statistical methods. The validity of the approach was supported by

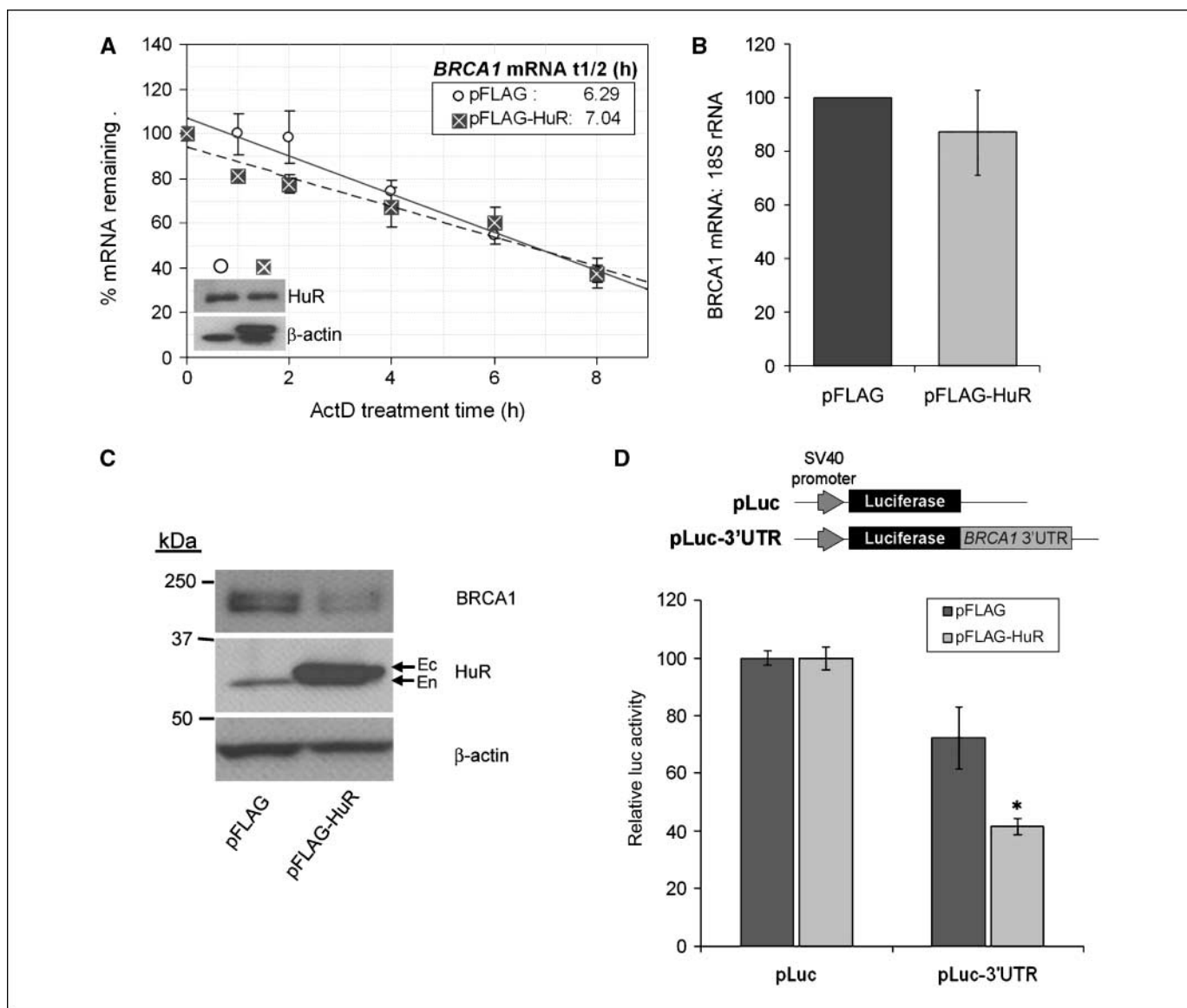


Figure 5. HuR regulates *BRCA1* posttranscriptionally and confers negative regulatory activity on the *BRCA1* 3'UTR. **A**, *BRCA1* mRNA stability assay in HeLa cells transiently transfected with empty pFLAG vector or a pFLAG-HuR expression construct. Transfectants were treated with the transcription inhibitor ActD for 0, 1, 2, 4, 6, or 8 h, then whole cell RNA was analyzed for *BRCA1* mRNA levels relative to 18S rRNA by Northern analysis. Blots were quantified by phosphorimaging, and the results are presented as *BRCA1*:18S ratios relative to the amounts present at time 0 h. *BRCA1* mRNA half-life ($t_{1/2}$) was calculated by linear regression analysis as the time taken for half the original amount of mRNA to decay. Points, means from three different transfections; bars, SE. Inset, representative Western blot demonstrating expression of the FLAG-HuR protein. **B**, Northern analysis of *BRCA1* mRNA levels in HeLa cells transiently transfected with pFLAG or pFLAG-HuR. *BRCA1* mRNA level was quantitated relative to 18S rRNA by phosphorimaging. Columns, mean from three transfections; bars, SE. **C**, representative Western blot showing HuR and *BRCA1* protein expression in HeLa cells transiently transfected with 250 ng of pFLAG or pFLAG-HuR (per well of a 6-well plate). Endogenous (En) and ectopic, FLAG-tagged HuR (Ec) are indicated. β -Actin was used as a protein loading control. Molecular mass is shown in kDa. **D**, *BRCA1* 3'UTR regulatory activity reporter assay. HeLa cells were transiently transfected with empty pFLAG or pFLAG-HuR, plus either empty pLuc reporter plasmid (containing the *Firefly* luciferase coding sequence) or a 3'UTR reporter construct (pLuc-3'UTR; containing the full-length *BRCA1* 3'UTR cloned immediately downstream of luciferase). Firefly luciferase activity was determined relative to a cotransfected *Renilla* luciferase internal control and expressed as a percentage of the matching pLuc empty vector control. Columns, mean of four independent experiments; bars, SDs. *P* values were determined with a two-tailed *t* test. *, *P* < 0.0001 compared with pFLAG in pLuc-3'UTR-transfected cells.

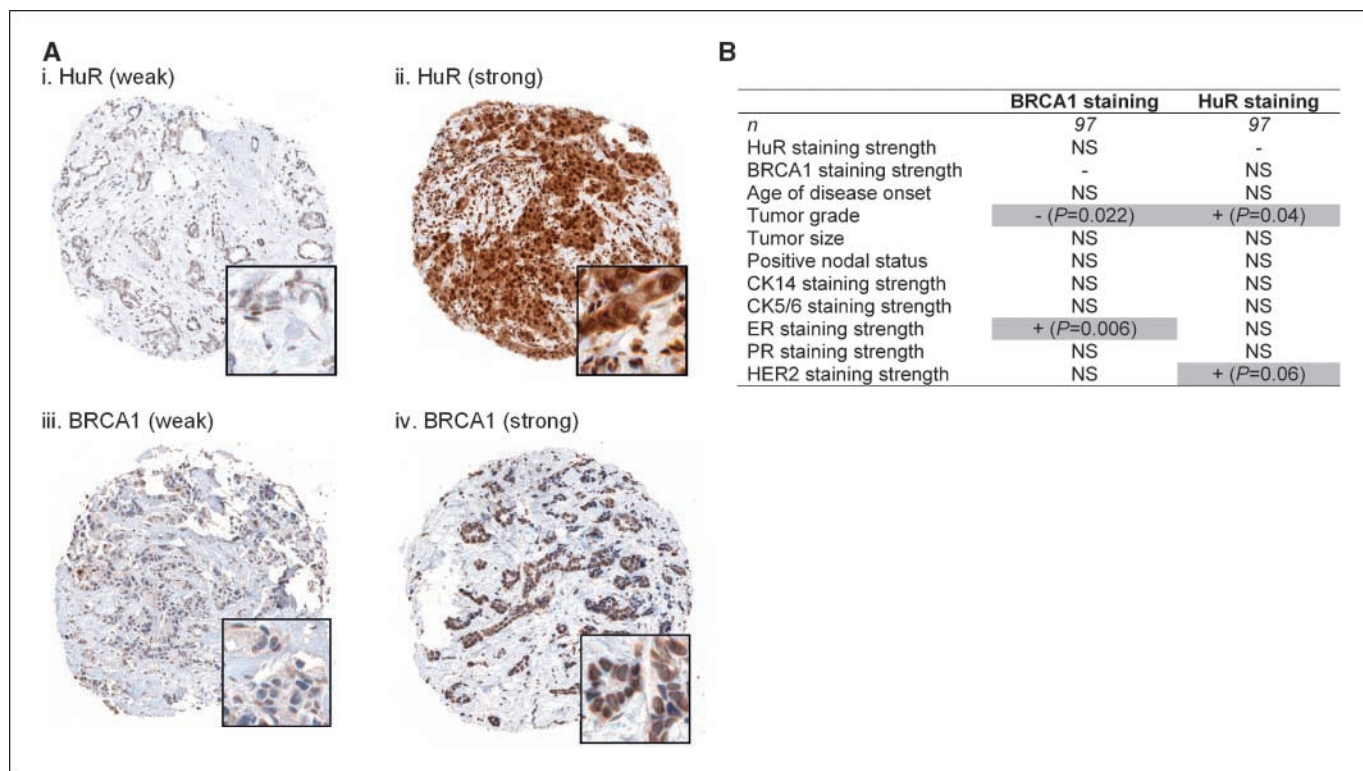


Figure 6. Association between BRCA1 protein expression or HuR protein expression and clinicopathologic features. *A*, example TMA cores showing weak (*A* and *C*) and strong (*B* and *D*) IHC staining for HuR (*i* and *ii*) and BRCA1 (*iii* and *iv*) in human breast ductal carcinoma tissue (magnification, $\times 60$; with inset, $\times 200$). TMAs were counter-stained with light haematoxylin. *B*, all features listed were incorporated into a multiple linear regression model using the IHC staining score for BRCA1 or HuR as the dependent variable. Sample population sizes (*n*), positive (+), inverse (-), or not significant (*NS*) *P* values are shown. *P* values of <0.05 were considered to be significant. *PR*, progesterone receptor.

finding some previously reported associations, including an association between *BRCA1* and ER (42) and an association between HuR and tumor grade (29, 30).

Comparison of HuR and BRCA1 in all tumors however revealed no statistically significant correlation. It is possible that the tumor cohort analyzed in this study is not large enough to give sufficient power to identify all significant association between our expression data and patient and tumor characteristics. The lack of association between BRCA1 expression and tumor grade supports this. Therefore, it will be interesting to see whether any association between BRCA1 and HuR is observed in future studies using larger cohorts of patients. It is also possible that HuR is not associated with BRCA1 expression in a causative relationship in breast cancer and that they are instead important independent collaborating contributors to initiation and/or progression of sporadic breast tumors.

An alternative hypothesis is that HuR does down-regulate BRCA1 expression *in vivo*, which would contribute to tumorigenesis, but that this only occurs in the early stages of breast cancer development. Once this tumorigenic event has occurred, other *BRCA1* regulators or events could simultaneously be induced in an attempt to compensate for *BRCA1* loss, resulting in reestablishment of *BRCA1* expression and, hence, the loss of association between the two proteins in end-stage tumors. That germline mutations in *BRCA1* confer susceptibility to breast cancer (1) is evidence that defects in *BRCA1* contribute to early event in breast tumorigenesis. Furthermore, tumors arising in *BRCA1* mutation carriers, which later acquire resistance to platinum compounds, do so by reestablishing *BRCA1* expression through secondary mutations (43), supporting the notion that sustained loss of *BRCA1* is not required for tumor

maintenance. Considering these factors, the lack of correlation of expression may not be informative in terms of the role of HuR in BRCA1-mediated tumorigenesis and, thus, does not necessarily reduce the significance of the functional relationship between these two molecules. Generation and analysis of mouse models in which HuR is overexpressed specifically in the mammary gland may enable this hypothesis to be further addressed in the future.

In summary, we show for the first time that HuR binds to a conserved HuR binding site in the *BRCA1* 3'UTR and that HuR posttranscriptionally regulates BRCA1 expression. Given the key role of *BRCA1* in breast tumorigenesis, further studies to fully elucidate the role of posttranscriptional regulation in the expression of *BRCA1* mRNA, including defining the precise role of HuR and other *trans*-acting molecules, will provide considerable insight into the mechanisms underlying development of breast cancer.

Disclosure of Potential Conflicts of Interest

No potential conflicts of interest were disclosed.

Acknowledgments

Received 4/15/2008; revised 8/18/2008; accepted 8/26/2008.

Grant support: Cancer Council of Victoria, The National Health and Medical Research Council of Australia (grants #143037, #401651, and #007011) and The UQ Foundation. J.D. French was supported by a National Breast Cancer Foundation Postdoctoral Training Fellowship.

The costs of publication of this article were defrayed in part by the payment of page charges. This article must therefore be hereby marked *advertisement* in accordance with 18 U.S.C. Section 1734 solely to indicate this fact.

We thank Joanne Bowles, Peter Boag, and Henry Furneaux for the reagents; Dick Wettenhall and Joe Rothnagel for valuable discussions; and Aisha Sauer, Anja Schmidtke, and Alex Gason for technical contributions.

References

1. Venkitaraman AR. Cancer susceptibility and the functions of BRCA1 and BRCA2. *Cell* 2002;108:171-82.
2. Vaughn JP, Davis PL, Jarboe MD, et al. BRCA1 expression is induced before DNA synthesis in both normal and tumor-derived breast cells. *Cell Growth Diff* 1996;7:711-15.
3. Saunus JM, Edwards SL, French JD, Smart CE, Brown MA. Regulation of BRCA1 messenger RNA stability in human epithelial cell lines and during cell cycle progression. *FEBS Letters* 2007;581:3435-42.
4. Wilson CA, Ramos L, Villaseñor MR, et al. Localization of human BRCA1 and its loss in high-grade, non-inherited breast carcinomas. *Nature Genet* 1999;21:236-40.
5. Brown MA, Lo J, Catteau A, et al. Germline BRCA1 promoter deletions in UK and Australian familial breast cancer patients: identification of a novel deletion consistent with BRCA1-yBRCA1 recombination. *Human Mutation* 2002;19:1-8.
6. Wang A, Schneider-Broussard R, Kumar AP, MacLeod MC, Johnson DG. Regulation of BRCA1 expression by the Rb-E2F pathway. *J Biol Chem* 2000;275:4532-36.
7. Rice JC, Futscher BW. Transcriptional repression of BRCA1 by aberrant cytosine methylation, histone hypoacetylation and chromatin condensation of the BRCA1 promoter. *Nucl Acids Res* 2000;28:3233-39.
8. Miyamoto K, Fukutomi T, Asada K, et al. Promoter methylation and post-transcriptional mechanisms for reduced BRCA1 immunoreactivity in sporadic human breast cancers. *Japanese J Clin Oncol* 2002;32:79-84.
9. Balmer LA, Beveridge DJ, Jazayeri JA, Thomson AM, Walker CE, Leedman PJ. Identification of a novel AU-rich element in the 3' untranslated region of epidermal growth factor receptor mRNA that is the target for regulated RNA-binding proteins. *Mol Cell Biol* 2001;21:2070-84.
10. Dean JLE, Wait R, Mahtani KR, Sully G, Clark AR, Saklatvala J. The 3' untranslated region of tumor necrosis factor α mRNA is the target of the mRNA-stabilizing factor HuR. *Mol Cell Biol* 2001;21:721-30.
11. Voelkerding KV, Steffen DW, Zaidi SH, Malter JS. Post-transcriptional regulation of the p53 tumor suppressor gene during growth-induction of human peripheral blood mononuclear cells. *Oncogene* 1995;10:515-21.
12. Giles KM, Daly JM, Beveridge DJ, et al. The 3'-untranslated region of p21WAF1 mRNA is a composite cis-acting sequence bound by RNA-binding proteins from breast cancer cells, including HuR and poly(C)-binding protein. *J Biol Chem* 2003;278:2937-46.
13. Moore MJ. From birth to death: the complex lives of eukaryotic mRNAs. *Science* 2005;309:1514-8.
14. Shabalina SA, Ogurtsov AY, Lipman DJ, Kondrashov AS. Patterns in interspecies similarity correlate with nucleotide composition in mammalian 3'UTRs. *Nucl Acids Res* 2003;31:5433-39.
15. Chen CY, Shyu AB. AU-rich elements: characterization and importance in mRNA degradation. *Trends Biochem Sci* 1995;20:465-70.
16. Bakheet T, Frevel M, Williams BRG, Greer W, Khabar KSA. ARE1: human AU-rich element-containing mRNA database reveals an unexpectedly diverse functional repertoire of encoded proteins. *Nucl Acids Res* 2001;29:246-54.
17. Kilav R, Silver J, Naveh-Manly TA. A conserved cis-acting element in the parathyroid hormone 3'-untranslated region is sufficient for regulation of RNA stability by calcium and phosphate. *J Biol Chem* 2001;276:8727-33.
18. Wiklund L, Sokolowski M, Carlsson A, Rush M, Schwartz S. Inhibition of translation by UAUUUU and UAUUUUUU motifs of the AU-rich RNA instability element in the HPV-1 late 3' untranslated region. *J Biol Chem* 2002;277:40462-71.
19. Shestakova EA, Singer RH, Condeelis J. The physiological significance of β -actin mRNA localization in determining cell polarity and directional motility. *Proc Natl Acad Sci U S A* 2001;98:7045-50.
20. Mignone F, Gissi C, Liuni S, Pesole G. Untranslated regions of mRNAs. *Genome Biol* 2002;3:Reviews0004.
21. Sobczak K, Krzyzosiak WJ. Structural determinants of BRCA1 translational regulation. *J Biol Chem* 2002;277:17349-58.
22. Signori E, Bagni C, Papa S, et al. A somatic mutation in the 5'UTR of BRCA1 gene in sporadic breast cancer causes down-modulation of translation efficiency. *Oncogene* 2001;20:4596-00.
23. Sengupta S, Jang BC, Wu MT, Paik JH, Furneaux H, Hla T. The RNA-binding protein HuR regulates the expression of cyclooxygenase-2. *J Biol Chem* 2003;278:25227-33.
24. Mazan-Mamczarz K, Galban S, Lopez de Silanes I, et al. RNA-binding protein HuR enhances p53 translation in response to ultraviolet light irradiation. *Proc Natl Acad Sci U S A* 2003;100:8354-59.
25. Wang W, Caldwell MC, Lin S, Furneaux H, Gorospe M. HuR regulates cyclin A and cyclin B1 mRNA stability during cell proliferation. *EMBO J* 2000;19:2340-50.
26. Kullmann M, Gopfert U, Siewe B, Hengst L. ELAV/Hu proteins inhibit p27 translation via an IRES element in the p27 5'UTR. *Genes Dev* 2002;16:3087-99.
27. Lopez de Silanes I, Zhan M, Lal A, Yang X, Gorospe M. Identification of a target RNA motif for RNA-binding protein HuR. *Proc Natl Acad Sci U S A* 2004;101:2987-92.
28. Lopez de Silanes I, Fan J, Yang X, et al. Role of the RNA-binding protein HuR in colon carcinogenesis. *Oncogene* 2003;22:7146-54.
29. Denkert C, Weichert W, Pest S, et al. Overexpression of the embryonic-lethal abnormal vision-like protein HuR in ovarian carcinoma is a prognostic factor and is associated with increased cyclooxygenase 2 expression. *Cancer Res* 2004;64:189-95.
30. Denkert C, Weichert W, Winzer KJ, et al. Expression of the ELAV-like protein HuR is associated with higher tumor grade and increased cyclooxygenase-2 expression in human breast carcinoma. *Clin Cancer Res* 2004;10:5580-86.
31. Heinonen M, Bono P, Narko K, et al. Cytoplasmic HuR expression is a prognostic factor in invasive ductal breast carcinoma. *Cancer Res* 2005;65:2157-61.
32. Erkinheimo TL, Lassus H, Sivula A, et al. Cytoplasmic HuR expression correlates with poor outcome and with cyclooxygenase 2 expression in serous ovarian carcinoma. *Cancer Res* 2003;63:7591-94.
33. Dixon DA, Tolley ND, King PH, et al. Altered expression of the mRNA stability factor HuR promotes cyclooxygenase-2 expression in colon cancer cells. *J Clin Invest* 2001;108:1657-65.
34. Heinonen M, Fagerholm R, Aaltonen K, et al. Prognostic role of HuR in hereditary breast cancer. *Clin Cancer Res* 2007;13:6959-63.
35. Wardrop S, kConFab, Brown MA. Identification of functional regulatory elements in intron 2 of the BRCA1 gene. *Genomics* 2005;86:316-28.
36. Altschul SF, Gish W, Miller W, Myers EW, Lipman DJ. Basic local alignment search tool. *J Mol Biol* 1990;215:403-10.
37. Hofacker IL. Vienna RNA secondary structure server. *Nucl Acids Res* 2003;31:3429-31.
38. French JD, Dunn J, Smart CE, Manning N, Brown MA. Disruption of BRCA1 function results in telomere lengthening and increased anaphase bridge formation in immortalized cell lines. *Genes Chromosomes Cancer* 2006;45:277-89.
39. Ostareck-Lederer A, Ostareck DH, Standart N, Thiele BJ. Translation of 15-lipoxygenase mRNA is inhibited by a protein that binds to a repeated sequence in the 3' untranslated region. *EMBO J* 1994;13:1476-81.
40. Leandersson K, Riesbeck K, Andersson T. Wnt-5a mRNA translation is suppressed by the Elav-like protein HuR in human breast epithelial cells. *Nucl Acids Res* 2006;34:3988-99.
41. Dormoy-Raclet V, Ménard I, Clair E, et al. The RNA-binding protein HuR promotes cell migration and cell invasion by stabilizing the β -actin mRNA in a U-rich-element-dependent manner. *Mol Cell Biol* 2007;27:5365-80.
42. Hosey AM, Gorski JJ, Murray MM, et al. Molecular basis for estrogen receptor α deficiency in BRCA1-linked breast cancer. *J Natl Cancer Inst* 2007;99:1683-94.
43. Swisher EM, Wataru Sakai W, Beth Y, et al. Secondary BRCA1 mutations in BRCA1-mutated ovarian carcinomas with platinum resistance. *Cancer Res* 2008;68:2581-86.